China Instrument and Control Society
Instrumentation
OPEN ACCESS
INSTRUMENTATION, Vol. 12, No. 4, December 2025 https://doi.org/10.15878/j.instr.202500319

Perspective

Axial-Flow-Induced Vibration Studies on Cantilever Rods for Nuclear Reactor Applications: A Summary of Recent Research

Andrea Cioncolini[1*], Mostafa R.A. Nabawy[2,3], Hao Li[4], Hector Iacovides[2]

[1] Department of Mechanical Engineering (Robotics), Guangdong Technion - Israel Institute of Technology, Shantou 515063, China

[2] Department of Mechanical and Aerospace Engineering, University of Manchester, Manchester M13 9PL, UK

[3] Aerospace Engineering Department, Faculty of Engineering, Cairo University, Giza 12613, Egypt

[4] School of Transportation Science and Engineering, Beihang University, Beijing 100191, China

[*] Corresponding author email: andrea.cioncolini@gtiit.edu.cn

Abstract: A frequent cause of unplanned and costly outages in water-cooled nuclear power plants is the premature failure of the fuel rods due to excessive flow-induced vibration in the reactor core. Turbulence and unsteadiness in the coolant water flowing through the reactor core can cause excessive vibration of the fuel rods, which in turn can result in fretting wear that eventually leads to the fuel rod cladding perforation and subsequent failure. The economic burden of unplanned reactor outages has motivated extensive research into flow-induced vibration. This perspective article provides a brief summary of recent research on flow-induced vibration of cantilever rod systems, which are simplified paradigmatic test configurations that have been instrumental to advance the fundamental physical understanding of axial-flow-induced vibration problems, and have enabled the development of cost-effective numerical methodologies for the simulation of these problems in engineering, with particular application to nuclear reactor systems. This summary covers recent experimental and numerical studies, and includes a description of a novel non-contact Hall-effect-based measuring technique specifically developed to track the vibration of the cantilever rod with gas-liquid two-phase flows. The article concludes by highlighting promising avenues for future research.

Keywords: optical tracking, hall-effect-based position tracking, particle image velocimetry (PIV), fluid-structure interaction (FSI)

Citation: Andrea Cioncolini, Mostafa R.A. Nabawy, Hao Li, Hector Iacovides."Axial-Flow-Induced Vibration Studies on Cantilever Rods for Nuclear Reactor Applications: A Summary of Recent Research." Instrumentation 12, no.4 (December 2025). https://doi.org/10.15878/j.instr.202500319

1 Introduction

Nuclear power plays a key role in global energy production, particularly as a source of low-carbon electricity. In fact, currently there are over 400 operating nuclear power reactors worldwide, with a combined electricity generation capacity of around 400 GW accounting for 10% of the global electricity production, and for 25% of the world's low-carbon supply. These figures make nuclear power the second-largest source of low-carbon electricity after hydroelectric power[1,2]. Driven by industrial development and population growth, the global energy demand is projected to increase substantially in the coming decades. The global electricity consumption, in particular, is expected to increase by over 80% by 2050[3], driven by the electrification of the industrial sector where electricity will gradually replace fossil fuels[4-7], by the increasing use of electric vehicles that will gradually replace fuel-powered ones[8-10], by the growth in air conditioning use due to increasing urbanization and rising global temperatures[11-13], and by the realization of data centres

for AI-driven applications[14,15]. In this scenario of increasing energy demand, nuclear power will remain a key player for low-carbon electricity generation: presently, in fact, there are 66 nuclear reactors under construction worldwide, while 85 more reactors are in the planning stage and an additional 344 reactor have been proposed[16-19]. In China, in particular, where carbon neutrality will be achieved by 2060, there are 58 operating nuclear reactors, 30 nuclear reactors are currently under construction, 36 units are in the planning stage, and 158 more have been proposed[16].

The vast majority of the nuclear power reactors currently operating, under construction, or in the planning stage worldwide, are water-cooled designs where the reactor core is cooled by water, with pressurized water reactors (PWRs) being the most prevalent[20,21]. In PWRs, the reactor core comprises thousands of fuel rods, which are slender (about 10 mm in diameter and 4 metres long) tubes made of a zirconium-based alloy that accommodate the uranium dioxide pellets where the fission reaction takes place to generate heat[22,23]. The fuel rods are arranged vertically inside the reactor core, and are cooled by high-pressure (15 MPa) water flowing upwards inside the core through the gaps between adjacent fuel rods. After passing through the reactor core, the coolant water is pumped into a steam generator where heat is transferred to a secondary water flow that evaporates producing pressurized steam. This latter is fed to a steam turbine that drives an electrical generator connected to the electric power grid. PWRs are designed to run continuously 24 hours a day and 7 days a week, and are only stopped for refuelling and maintenance. A refuelling outage typically lasts 3-4 weeks and takes place at intervals of 12, 18, or 24 months when a quarter to a third of the fuel rods in the reactor core are replaced with fresh ones.

Unplanned reactor outages involve a costly loss of electricity production (on the order of €1M/day for a 1 GW reactor) and are highly detrimental to the profitability of the power plant. A frequent cause of unplanned PWR outages over the last years has been the premature failure of the fuel rods due to flow-induced vibration (FIV) in the reactor core, which is more specifically termed 'axial-FIV' on account of the fact that the coolant flow inside the reactor core is directed axially along the lateral surface of the fuel rods[24,25]. Specifically, turbulence and unsteadiness in the coolant water flowing through the reactor core can cause an excessive vibration of the fuel rods, which in turn can result in fretting wear localized at the points of contact of the fuel rods with the supporting structures present inside the reactor core. The progressive thinning of the cladding of the fuel rod caused by the fretting wear eventually leads to the cladding perforation and, consequently, to the premature failure of the fuel rod. Such an occurrence does not pose any risks to the environment or the population, but does require an unplanned and costly reactor outage to replace the faulty fuel rod(s) with fresh ones. The economic burden of unplanned outages has motivated extensive research in recent years with a view to better understand the multi-disciplinary physics of axial-FIVs, which combines fluid mechanics with solid mechanics and that is further complicated by the strong coupling between fluid flow and structural vibration. A solid fundamental physical understanding of axial-FIV would translate into more accurate and reliable numerical simulation tools, which in turn would enable designing more durable nuclear fuel rods.

This perspective article provides a brief summary of the research carried out recently on axial-FIVs employing cantilever rod systems, which are paradigmatic test configurations that, despite their simplicity, incorporate the relevant physics of the axial-FIV phenomenon. The knowledge accumulated with cantilever rod systems has enhanced our fundamental physical understanding of axial-FIVs, and has enabled the development of cost-effective numerical methodologies that are capable of successfully reproducing the experimental observations. These numerical methodologies are still in the development stage. Being easily scalable, once perfected these methodologies will enable the analysis of axial-FIVs with more complex multirod configurations operating under high pressure and high temperature conditions of direct relevance to nuclear engineering applications, where experimental investigations become expensive and often impractical. In the future, these numerical methodologies hold promise of being incorporated into nuclear fuel design methodologies, to support the design of more fatigue resistant and durable nuclear fuel rods.

2 Axial-FIV of Cantilever Rods

The economic burden of unplanned reactor outages has motivated extensive research into axial-FIVs, with recent experimental studies focusing on simplified test configurations that incorporate a single cantilever rod confined inside a tube and exposed to a flow of water directed axially inside the confining tube along the cantilever rod. Despite the absence of the rod-to-rod interaction and of the support structures present in nuclear reactor cores, and therefore the absence of fretting wear, the sources of excitation present in cantilever rod configurations are broadly the same as those present in actual reactor cores, namely flow unsteadiness, turbulent buffeting, and excitation due to the movement of the rods. Therefore, by combining a rich physics with design simplicity, cantilever rod setups constitute a paradigmatic test case that has proved instrumental in advancing the fundamental physical understanding of axial-FIVs[26-33], and has also provided invaluable high-resolution data for the subsequent development and validation of numerical simulation methodologies[34-40].

A representative example of a cantilever rod test section is provided in Fig. 1a. The test setup is briefly described below, while a more comprehensive description can be found in[31]. The setup is vertically oriented and comprises a cantilever rod confined inside a pipe that is rigidly connected to a fixed support frame (not shown in the Figure). The dimensions of the cantilever rod (8.83/10.01 mm inner/outer diameter, moment of inertia of the cross section of 194 mm^4, and 1045 mm overhang length) and confining tube (20.86 mm inner diameter) have been selected to be representative of PWR fuel rods; in particular, the hydraulic diameter of the annular flow passage between confining tube and cantilever rod is of 10.85 mm, a figure close in value to the hydraulic diameter of PWR nuclear reactor cores. The cantilever rod is made of stainless-steel piping (SS AISI 316, with Young's modulus of 193 GPa) and is filled with lead shot (density of 11.3 g/cm^3) to mimic the loading of uranium dioxide fuel pellets (density of 10.97 g/cm^3); the lead shot filling yields a linear mass density for the cantilever rod of 588 g/m. The confining tube is made of stainless-steel and incorporates a transparent section, located at the same elevation of the cantilever rod tip, that provides optical access for rod vibration detection and flow field visualization (see Fig 1 and Fig 2a). The transparent section, which is made of Perspex piping matching in diameter the confining tube, is surrounded by a square Perspex tube, and the gap between Perspex square tube and Perspex pipe is filled with water during the tests to eliminate the optical distortion caused by the curvature of the tube. The cantilever rod test section is incorporated into a hydraulic flow loop that, as schematically shown in Fig 1b, comprises a water tank reservoir, a flow circulation pump, a flow meter, and a water temperature sensor.

Water flow enters at the bottom of the test section and exits at the top, as indicated in Fig. 1a (upflow condition), or vice versa it enters at the top and exits at the bottom (downflow condition). During the tests, which were carried out at ambient temperature (285-295 K) and pressures of 200-300 kPa, the flow loop can provide water flow rates from 0.2 kg/s up to about 2.5 kg/s, corresponding to an average flow velocity through the test section from 0.7 m/s up to 8-9 m/s that translates into Reynolds number values from 10k up to about 100k-120k, hence ensuring fully turbulent flow conditions during the tests. Turbulence and unsteadiness in the water flow excite the cantilever rod that starts to vibrate; once the amplitude of the vibration is large enough, the motion of the rod affects the flow, thus providing an additional source of excitation (so-called movement-induced excitation). A further source of excitation is given by the flow separation localized around the rod tip, which configures a localized unsteadiness in the flow. The average flow velocity in PWR cores is 4-5 m/s, which is a range of values well within the capability of the cantilever rod setup. On account of the difference in the

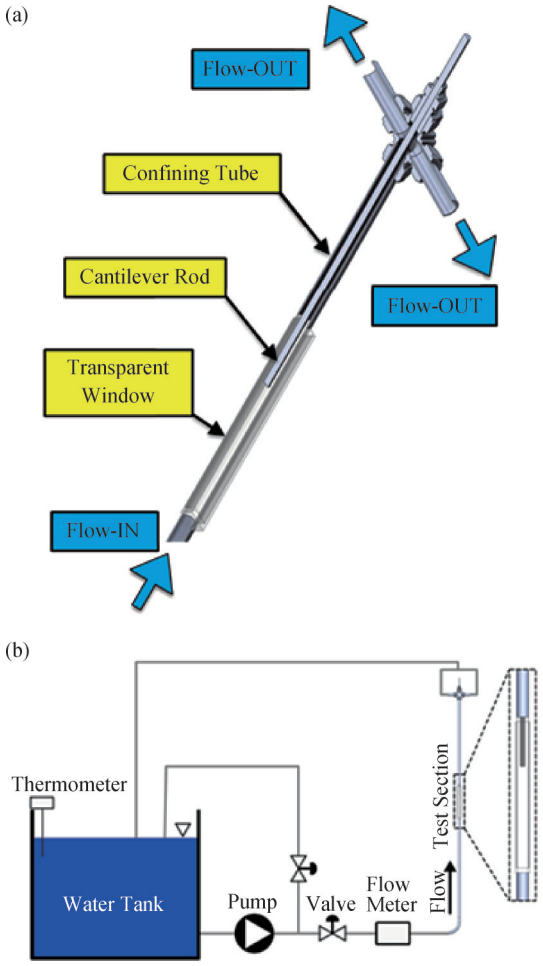

Fig.1 a) Representative example of a cantilever rod test piece employed in axial-FIV studies for nuclear reactor applications, comprising a cantilever rod confined inside a tube with a matching-diameter transparent window for optical access; and b) sketch of the hydraulic flow loop employed to run the experiments, comprising a water tank, a flow circulation pump, a flow meter, and a water thermometer (further details in[31]).

values of density and viscosity of water at ambient temperature and PWR operating temperature (about 600 K), the Reynolds number in PWR cores is on the order of 400k-500k; hence, about 4-5 times larger than the Reynolds number values achieved in the cantilever rod setup. In spite of this limitation, the physical mechanisms responsible for the axial-FIV, namely turbulence, flow unsteadiness and separation, and movement-induced excitation, are largely the same in PWR cores and in the cantilever rod setup, making this latter a useful and informative paradigmatic test configuration.

The rod vibration was measured with non-contact optical imaging and tracking. Specifically, the vibration of the cantilever rod free-end was recorded with a Panasonic Lumix DMC-FZ200 digital camera with image resolution of 1280×720 pixels, spatial resolution of about 10 pixel/mm and position tracking accuracy of ±0.1 pixel corresponding to ±10 μm, recording frequency of 100 fps, and recording duration of 60 s (further details in[31]). The dominant rod vibration frequency is on the order of

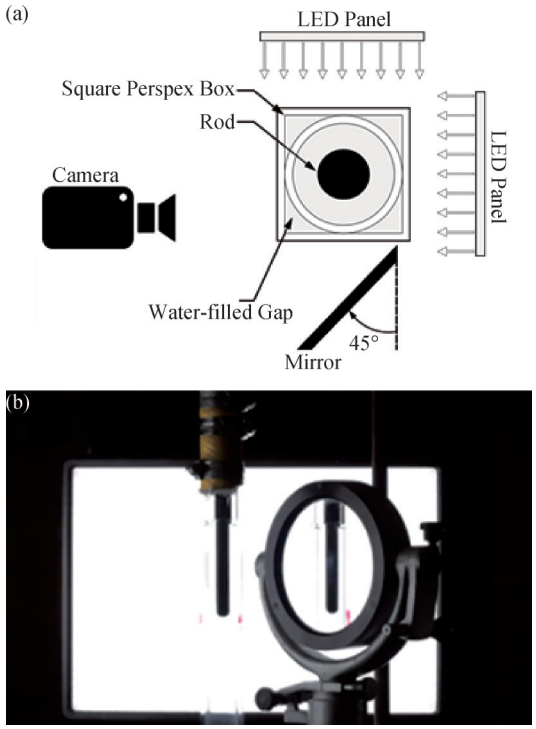

Fig.2 a) Schematic representation of the optical setup for measuring the cantilever rod vibration, comprising a fast video camera with a mirror for detecting the rod vibration in 3D and LED back lighting; and b) a representative raw image captured by the camera (further details in[31,32]).

3-7 Hz, hence a recording frequency of 100 fps is adequate, and a recording time of 60 s is sufficient to obtain representative averages. The camera was placed facing the test piece as indicated in Fig. 2a. The optical setup incorporated a mirror positioned to the side of the test section and inclined at 45 degrees, so that the camera could record simultaneously both a frontal and a lateral view of the vibrating rod free-end (see Fig. 2b), hence enabling the reconstruction of the rod vibration in 3D. Clearly, the same result could have been achieved by employing two cameras, oriented so as to look at the test setup from orthogonal directions. The single-camera setup is more cost-effective and eliminates the trouble of synchronizing multiple videos. Note that, on account of the small diameter of the cantilever rod and the absence of free space inside it (the rod is filled with lead shot, as commented previously), accelerometers are not suitable for the present application.

The image processing and the subsequent rod displacement time-series analysis were carried out with an in-house-made object tracking methodology implemented with the free software GNU Octave version 4.2.2, employing built-in features provided in the packages 'image' and 'signal'. Specifically, the recorded images were binarized and complemented to isolate one single feature corresponding to the cantilever rod free-end tip, whose centroid was then computed and recorded to assemble the time-series for the frontal and lateral rod displacement. These were then analyzed by computing the power spectrum, the autocorrelation function, and the reconstructed attractor in phase-space[41].

The power spectrum, in particular, was computed from the raw time-series using the well-known method of Welch (function *pwelch* in GNU Octave), whereas the noise in the time-series was reduced using a 13-point Henderson moving-average filter before computing the autocorrelation function and the reconstructed attractor in phase-space. When employed jointly, the power spectrum, the autocorrelation function, and the reconstructed attractor in phase-space provide a thorough characterization of the cantilever rod vibration. A representative example is provided in Fig. 3, which provides a 5 s long sample of the frontal displacement time-series (Fig. 3a) together with its power spectrum that presents one dominant vibration peak (Fig. 3b), its autocorrelation function that is periodic and slowly decaying (Fig. 3c), and the reconstructed attractor that is ring-shaped (Fig. 3d): these features indicate a large-amplitude flutter-like periodic vibration. The corresponding rod motion in 3D is shown in Fig. 4a for the entire 60 s long time-series, together with its projection onto the horizontal plane in Fig. 4b which further indicates that the large-amplitude flutter-like rod vibration comprises a rotation around the vertical axis with a superimposed slower rotation of the axis itself, i.e., a precession of the rod tip motion. Further details on the tracking methodology and more exhaustive experimental observations can be found in[31,32].

The flow field around the cantilever rod tip was visualized using a Dantec Dynamics particle image velocimetry (PIV) setup comprising a Litron LDY302 double-cavity laser (pulse duration of 10 ns and pulse energy of 15 mJ at a wavelength of 527 nm) and a Phantom V310 high-speed video camera operated in double-frame mode (image resolution of 1280×800 pixel and recording frequency of 200 Hz). For the visualization, the flow was seeded with hollow glass spheres with a nominal diameter of 10 μm. The flow field visualizations complete and integrate the cantilever rod vibration results previously described by providing details regarding the flow field around the rod tip, particularly flow separation and unsteadiness. Representative flow visualization results are presented in Fig. 5 for four different shapes of the cantilever rod tip (a blunt tip and three cones with height to diameter ratio of 0.5, 1, and 2) for upflow (Fig. 5a) and downflow (Fig. 5b) conditions at a Reynolds number value of 83k. As can be noted, the flow appears remarkably different for the four rod tip shapes, with a more pronounced flow separation for the blunt tip shape. More comprehensive flow visualisations can be found in[31,32].

The optical tracking methodology for the cantilever rod tip previously described is not applicable to gas-liquid two-phase flow conditions, because the gas-liquid interface present in the flow distorts and hides the rod tip, making the computation of the tip centroid inaccurate or

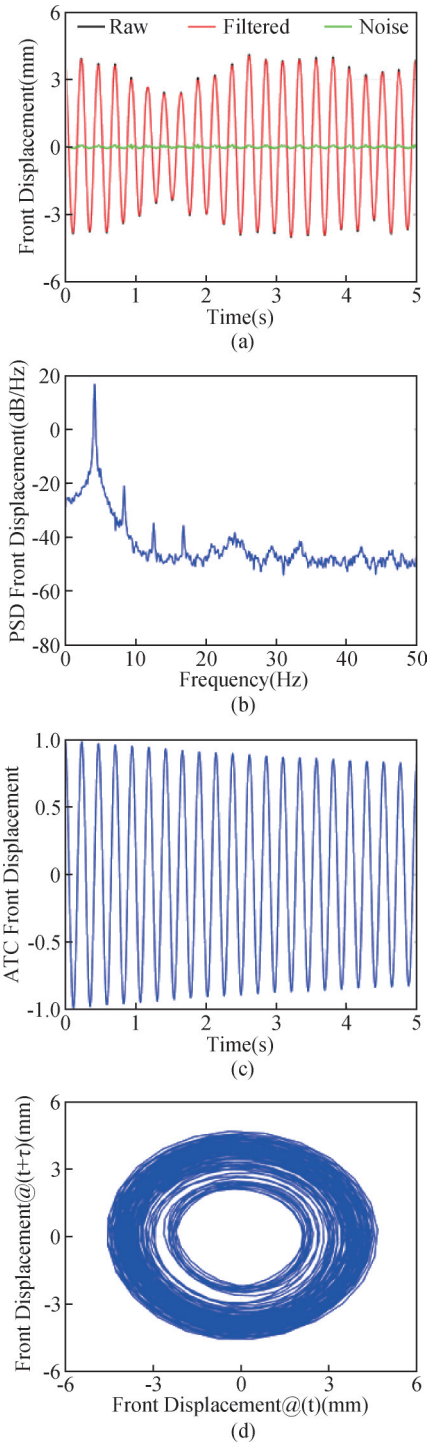

Fig. 3 Representative results for cantilever rod vibration, detected with downflow for a Reynolds number value of 49.1k, depicting a flutter-like large-amplitude periodic vibration: a) a 5 s long sample of the displacement time-series (position tracking accuracy of ±10μm); b) the power spectrum (PSD) of the displacement time-series, with one dominant vibration frequency at about 4 Hz; c) the autocorrelation function (ATC) of the displacement time-series, indicating periodic motion with slow decay; and d) the reconstructed attractor in phase-space, which appears ring-shaped hence indicating periodic motion (further details in[31]).

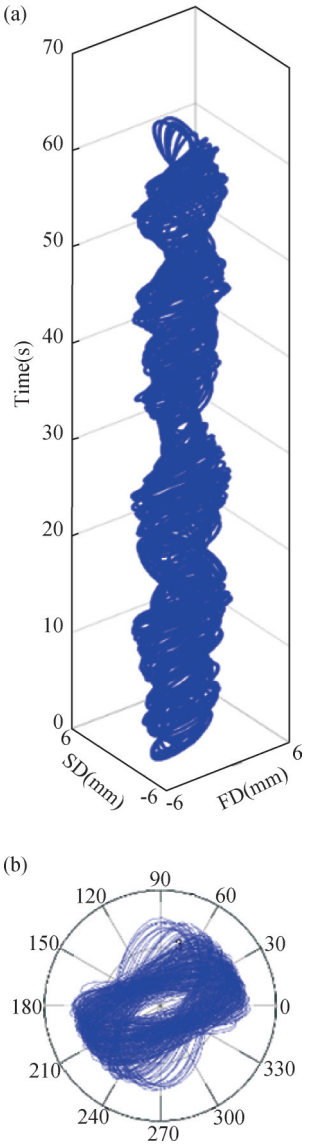

Fig.4 Representative results for cantilever rod vibration, detected with downflow for a Reynolds number value of 49.1k, depicting a flutter-like large-amplitude periodic vibration (see Fig. 3 and associated discussion): a) rod tip trajectory in 3D and b) rod tip trajectory projection onto the horizontal plane, indicating a rotation of the rod tip around the vertical axis of the rod with superimposed a slower rotation (a motion of precession) of the axis itself (further details in[31]).

impossible. Gas-liquid two-phase flow conditions are important for the operation of boiling water reactors (BWRs) where the coolant water evaporates as it flows through the reactor core, hence motivating the need for extending the cantilever rod testing methodology to two-phase flow conditions..

A novel Hall-effect-based tracking methodology that has recently been developed for two-phase flow applications is shown in Fig. 6[33]. The sensing setup comprises permanent magnets (RS PRO neodymium disc magnet with diameter of 4 mm) fixed at the tip of the cantilever rod, and four Hall-effect sensors (Honeywell SS495A) housed inside a 3D printed external block and located around the test piece. When the rod vibrates, the distance between the permanent magnets fixed at its tip and the Hall-effect sensors changes, thereby affecting the output of these latter. Once the setup is calibrated,

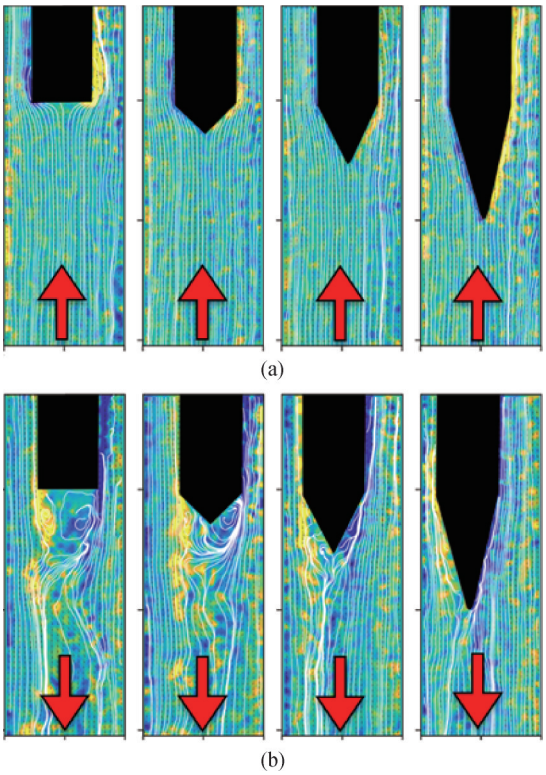

Fig.5 Representative results for velocity fields and streamlines measured with particle image velocimetry (PIV) for a Reynolds number value of 83k and: a) upflow; b) downflow (the arrows indicate the direction of the water flow), for four different shapes of the cantilever rod tip (a blunt tip and three cones with height to diameter ratio of 0.5, 1, and 2) (further details in[31,32]).

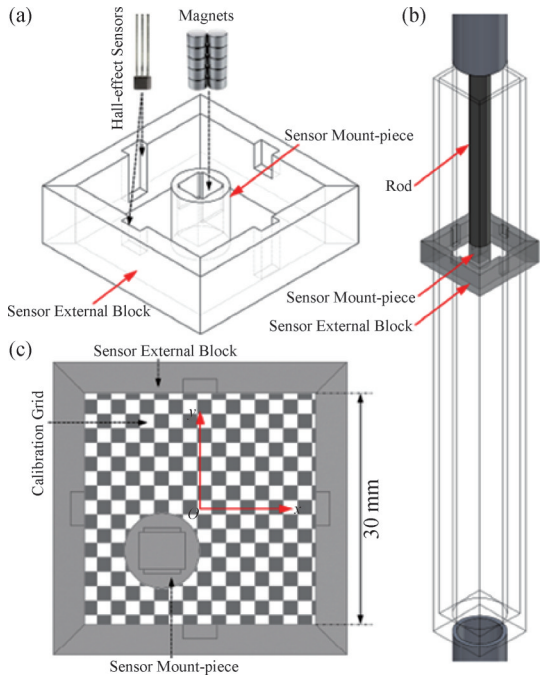

Fig.6 The Hall-effect-based tracking methodology developed for two-phase flow conditions where image tracking is not feasible: a) schematics of the sensing setup, comprising permanent magnets attached to the cantilever rod tip and four Hall-effect sensors located around the rod tip and placed inside a 3D printed external block; b) schematics of the installation of the sensor; and c) static calibration of the sensor, where the rod tip position is correlated to the Hall-effect sensors output enabling the reconstruction of the rod position from the signals of the Hall-effect sensors; rod tip position tracking accuracy: ±50μm (further details in[33]).

therefore, the output signals of the Hall-effect sensors can be employed to reconstruct the position of the cantilever rod tip. Clearly, the Hall-effect-based tracking methodology can also be employed with single-phase water flow, hence enabling a cross-comparison with the optical tracking methodology previously described, showing an accuracy of about ±50 μm in the tracking of the rod tip, which is adequate for the present application.

Besides enabling a better fundamental physical understanding of axial-FIV problems, the experimental results generated with cantilever rod setups (like those presented in Figs. 3-5) have also been instrumental for the development and validation of numerical simulation methodologies. A representative example of a numerical simulation that successfully reproduced the observed cantilever rod vibration is presented in Fig. 7. The numerical simulation was carried out with Solid4FOAM, which is a toolbox of the open-source software OpenFOAM specifically designed for fluid-structure interaction problems. Specifically, the simulation was carried out with a relatively coarse mesh (about 100k cells for the solid and 1M cells for the fluid) which produced mesh-independent results with limited computational cost, where the near-wall flow was not resolved (wall functions were employed), and the turbulence in the flow was modelled with the well-known URANS Reynolds Stress Model proposed by Launder,

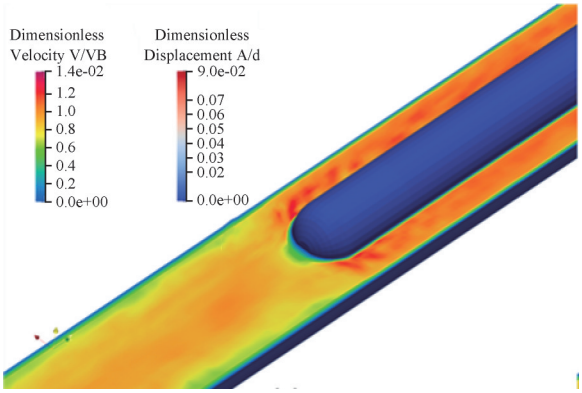

Fig.7 Representative results of numerical simulations that effectively reproduce the cantilever rod vibration observed in the experiments, generated with the software platform solid4Foam (an OpenFOAM toolbox for fluid-structure interactions) for upflow conditions (left-to-right in the figure) and a Reynolds number value of 16.8k (further details in[38]).

Reece and Rodi (LRR). The numerical methodology in extensively described in[38,39] where the governing equations for the fluid and the solid are provided, together with the interface coupling strategy, all relevant settings of the numerical model, and relevant validations. Both the amplitude and the frequency of the observed rod vibration were successfully reproduced in the numerical simulation. This is a remarkable outcome, considering the

cost-effectiveness of the numerical model, where the most critical aspect was the adoption of a turbulence model capable of reproducing sufficient unsteadiness in the flow to trigger and sustain the vibration. In addition, the validated numerical methodology was employed to carry out numerical experiments where the fluid flow and the rod elasticity were individually varied to better dissect their effects on the resulting FIV[38].

3 Conclusions and Outlook

This perspective article provided a brief overview of recent research carried out with cantilever rod systems, which have recently emerged as simple paradigmatic test configurations particularly suited to investigate the complex physics underpinning axial-FIVs. This has rather broad relevance in engineering, particularly for water-cooled nuclear reactor applications. The high-resolution data recently gathered with cantilever rod setups has enabled a better fundamental physical understanding of axial-FIV problems, and has also enabled the subsequent development of cost-effective numerical simulation methodologies that successfully reproduce the experimental observations. Areas where further experimental research would be beneficial include the following:

• Measurements carried out with test setups that incorporate multi-rod configurations, vith a view at characterizing rod-to-rod interactions;

• Measurements carried out with test setups that incorporate support structures conceived to allow a small relative movement between the vibrating rod and the support, similarly to what happens in actual nuclear fuel bundels, vith a view at measuring and characterizing fretting wear alongside the flow-structure interaction;

• Experiments carried out at higher flow velocity and operating temperature to extend the range of Reynolds number covered, ideally approaching the values typical of actual nuclear reactor cores;

• Experiments carried out with gas-liquid two-phase flow conditions, which is an area that has been only marginally explored, and that is relevant for boiling water nuclear reactors.

Following the same approach adopted in the recent experimental investigations with cantilever rod setups, future experiments should address simultaneously both the structural motion and the flow field, with a space/time resolution adequate for the susbequent development of the numerical simulation methodologies. Numerical modelling areas where further research would be beneficial include the folllowing:

• The implementation of efficient dynamic meshing strategies capable of effectively handling large structural displacements and solid-to-solid contact;

• The extension/validation of turbulence models capable of reproducing sufficient unsteadiness in the flow to trigger and sustain axial-FIVs.

In addition to water-cooled nuclear reactors, axial-FIVs are of relevance for liquid metal cooled nuclear reactors and for various other applications in engineering, includind pipes conveying fluids employed in ocean mining, pipes exposed to both internal and external flows used in fluid-power drilling, slender cylindrical structures towed in liquids of relevance in mineral exploration in deep sea, and high-speed trains.

Author Contribution:

Andrea Cioncolini: Conceptualization, Writing – original draft, Writing – review & editing; Mostafa R. A. Nabawy: Writing – review & editing, Hao Li: Writing – review & editing, Hector Iacovides: Writing – review & editing.

Funding Information:

This research received no external funding.

Data Availability:

Data sharing is not applicable to this article as no new data were created or analyzed in this study.

Conflicts of Interest:

The authors declare no competing interests.

Dates:

Received 18 August 2025; Accepted 16 November 2025; Published online 31 December 2025

References

[1] Nuclear Power Reactors in the World, International Atomic Energy Agency **2024**. https://www. iaea. org/publications/15748/nuclear-power-reactors-in-the-world

[2] Nuclear Power in the World Today, World Nuclear Association **2025**. https://world-nuclear. org/information-library/current-and-future-generation/nuclear-power-in-the-world-today

[3] World Energy Outlook **2024**, International Energy Agency (**2024**). https://www. iea. org/reports/world-energy-outlook-2024

[4] M. Wei, C. A. McMillan, S. De La Rue Du Can, Electrification of Industry: Potential, Challenges and Outlook. *Current Sustainable/Renewable Energy Reports* 6, 140-148 (**2019**). https://doi.org/10.1007/s40518-019-00136-1

[5] P. Sorknæs, R. M. Johannsen, A. D. Korberg, T. B. Nielsen, U. R. Petersen, B. V. Mathiesen, Electrification of the industrial sector in 100% renewable energy scenarios. *Energy* 254, 124339 (**2022**. https://doi.org/10.1016/j.energy.2022.124339

[6] D. S. Mallapragada, Y. Dvorkin, M. A. Modestino, D. V. Esposito, W. A. Smith, B. -M. Hodge, M. P. Harold, V. M. Donnelly, A. Nuz, C. Bloomquist, K. Baker, L. C. Grabow, Y. Yan, N. N. Rajput, R. L. Hartman, E. J. Biddinger, E. S. Aydil, A. D. Taylor, Decarbonization of the chemical industry through electrification: Barriers and opportunities. *Joule 7* ,

23-41 (**2023**). https://doi.org/10.1016/j.joule.2022.12.008

[7] S. Nadel, Electrification in the Transportation, Buildings, and Industrial Sectors: A Review of Opportunities, Barriers, and Policies. *Current Sustainable/Renewable Energy Reports* 6, 158-168 (**2019**). https://doi.org/10.1007/s40518-019-00138-z

[8] A. C. Ruoso, J. L. D. Ribeiro, D. Olaru, Electric vehicles' impact on energy balance: Three-country comparison. Renewable and Sustainable Energy Reviews 203, 114768 (**2024**). https://doi.org/10.1016/j.rser.2024.114768

[9] T. Nogueira, E. Sousa, G. R. Alves, Electric vehicles growth until **2030**: Impact on the distribution network power. *Energy Reports* 8, 145-152 (**2022**. https://doi. org/10.1016/j. egyr.2022.01.106

[10] M. Baronchelli, D. Falabretti, F. Gulotta, Power Demand Patterns of Public Electric Vehicle Charging: A 2030 Forecast Based on Real-Life Data. *Sustainability* 17, 1028 (2025). https://doi.org/10.3390/su17031028

[11] P. Sherman, H. Lin, M. McElroy, Projected global demand for air conditioning associated with extreme heat and implications for electricity grids in poorer countries. Energy and Buildings 268, 112198 (**2022**). https://doi. org/10.1016/j. enbuild.**2022**.112198

[12] G. G. Tocchio, I. D. M. Neto, R. C. Da Silva, R. S. De Lima, R. D. V. Salvo, R. M. Galante, R. N. Michels, Forecasting demand for air conditioning in the Brazilian residential sector. Journal of Building Engineering 96, 110572 (**2024**). https:// doi.org/10.1016/j.jobe.**2024**.110572

[13] L. W. Davis, P. J. Gertler, Contribution of air conditioning adoption to future energy use under global warming. *PNAS* 112, 5962-5967 (**2015**). https://doi.org/10.1073/pnas.1423558112

[14] S. Chen, How much energy will AI really consume? The good, the bad and the unknown. *Nature 639* , 22-24 (**2025**). https://doi.org/10.1038/d41586-025-00616-z

[15] A. De Vries, The growing energy footprint of artificial intelligence. *Joule* 7, 2191-2194 (**2023**). https://doi. org/ 10.1016/j.joule.2023.09.004

[16] Plans for New Reactors Worldwide, World Nuclear Association **2025**. https://world-nuclear. org/information-library/current-and-future-generation/plans-for-new-reactors-worldwide#:~:text=Today%20there%20are%20about%20440, 9%25%20of%20the%20world's%20electricity

[17] L. Liu, H. Guo, L. Dai, M. Liu, Y. Xiao, T. Cong, H. Gu, The role of nuclear energy in the carbon neutrality goal. Progress in Nuclear Energy 162, 104772 (**2023**). https://doi. org/ 10.1016/j.pnucene.**2023**.104772

[18] E. K. Addo, A. T. Kabo-bah, F. A. Diawuo, S. K. Debrah, The Role of Nuclear Energy in Reducing Greenhouse Gas (GHG) Emissions and Energy Security: A Systematic Review. *International Journal of Energy Research 2023* , 1-31 (**2023**). https://doi.org/10.1155/2023/8823507

[19] J. Bistline, S. Bragg-Sitton, W. Cole, B. Dixon, E. Eschmann, J. Ho, A. Kwon, L. Martin, C. Murphy, C. Namovicz, A. Sowder, Modeling nuclear energy's future role in decarbonized energy systems. iScience 26, 105952 (**2023**). https://doi.org/10.1016/j.isci.2023.105952

[20] Are there different types of nuclear reactor? World Nuclear Association. https://world-nuclear. org/nuclear-essentials/are-there-different-types-of-reactor

[21] Water Cooled Reactors, International Atomic Energy Agency. https://www.iaea.org/topics/water-cooled-reactors

[22] How is uranium made into nuclear fuel? World Nuclear Association. https://world-nuclear. org/nuclear-essentials/how-is-uranium-made-into-nuclear-fuel

[23] Physics of Uranium and Nuclear Energy, World Nuclear Association **2025**. https://world-nuclear. org/information-library/nuclear-fuel-cycle/introduction/physics-of-nuclear-energy

[24] Review of Fuel Failures in Water Cooled Reactors, International Atomic Energy Agency (2010) https://www.iaea.org/publications/8259/review-of-fuel-failures-in-water-cooled-reactors

[25] Z. Cai, Z. Li, M. Yin, M. Zhu, Z. Zhou, A review of fretting study on nuclear power equipment. Tribology International 144, 106095 (**2020**). https://doi.org/10.1016/j.triboint.2019.106095

[26] S. Rinaldi, M. P. Païdoussis, Theory and experiments on the dynamics of a free-clamped cylinder in confined axial air-flow. *Journal of Fluids and Structures* 28, 167-179 (**2012**). https://doi.org/10.1016/j.jfluidstructs.2011.07.006

[27] S. Rinaldi, M. P. Païdoussis, An improved theoretical model for the dynamics of a free-clamped cylinder in axial flow. Journal of Fluids and Structures 94, 102903 (**2020**). https:// doi.org/10.1016/j.jfluidstructs.**2020**.102903

[28] A. R. Abdelbaki, M. P. Païdoussis, A. K. Misra, A nonlinear model for a free-clamped cylinder subjected to confined axial flow. *Journal of Fluids and Structures* 80, 390-404 (**2018**). https://doi.org/10.1016/j.jfluidstructs.**2018**.03.006

[29] B. De Pauw, W. Weijtjens, S. Vanlanduit, K. Van Tichelen, F. Berghmans, Operational modal analysis of flow-induced vibration of nuclear fuel rods in a turbulent axial flow. *Nuclear Engineering and Design* 284, 19-26 (**2015**). https:// doi.org/10.1016/j.nucengdes.**2014**.11.040

[30] A. Cioncolini, J. Silva-Leon, D. Cooper, M. K. Quinn, H. Iacovides, Axial-flow-induced vibration experiments on cantilevered rods for nuclear reactor applications. *Nuclear Engineering and Design* 338, 102-118 (**2018**). https://doi.org/ 10.1016/j.nucengdes.2018.08.010

[31] A. Cioncolini, S. Zhang, M. R. A. Nabawy, H. Li, D. Cooper, H. Iacovides, Experiments on axial-flow-induced vibration of a free-clamped/clamped-free rod for light-water nuclear reactor applications. Annals of Nuclear Energy 190, 109900 (**2023**). https://doi.org/10.1016/j.anucene.2023.109900

[32] H. Li, A. Cioncolini, S. Zhang, H. Iacovides, M. R. A. Nabawy, Tip shape effects on the axial-flow-induced vibration of a cantilever rod. Journal of Fluids and Structures 127, 104132 (**2024**). https://doi. org/10.1016/j. jfluidstructs. 2024.104132

[33] H. Li, M. R. A. Nabawy, W. Benguigui, H. Iacovides, A. Cioncolini, Experiments on axial-flow-induced vibration of a cantilever rod in two-phase flow. AIAA SCITECH **2025**

Forum, 6-10 January **2025**, Orlando, FL, USA. https://doi.org/10.2514/6.2025-1687

[34] J. De Ridder, J. Degroote, K. Van Tichelen, P. Schuurmans, J. Vierendeels, Modal characteristics of a flexible cylinder in turbulent axial flow from numerical simulations. *Journal of Fluids and Structures* 43, 110-123 (**2013**). https://doi. org/10.1016/j.jfluidstructs.**2013**.09.001

[35] S. Kottapalli, A. Shams, A. H. Zuijlen, M. J. B. M. Pourquie, Numerical investigation of an advanced U-RANS based pressure fluctuation model to simulate non-linear vibrations of nuclear fuel rods due to turbulent parallel-flow. *Annals of Nuclear Energy* 128, 115-126 (**2019**). https://doi.org/10.1016/j.anucene.**2019**.01.001

[36] D. De Santis, A. Shams, An advanced numerical framework for the simulation of flow induced vibration for nuclear applications. *Annals of Nuclear Energy* 130, 218-231 (**2019**). https://doi.org/10.1016/j.anucene.**2019**.02.049

[37] J. Salachna, A. Cioncolini, H. Iacovides, Benchmark simulation of the flow-induced vibrations for nuclear applications. Annals of Nuclear Energy 180, 109425 (**2023**). https://doi.org/10.1016/j.anucene.**2022**.109425

[38] W. Mao, H. Iacovides, A. Cioncolini, H. Li, M. R. A. Nabawy, A validated numerical methodology for flow-induced vibration of a semi-spherical end cantilever rod in axial flow. Physics of Fluids 36, 075155 (**2024**). https://doi.org/10.1063/5.0211524

[39] A. Muhamad Pauzi, H. Iacovides, A. Cioncolini, H. Li, M. R. A. Nabawy, Application of URANS Simulation and Experimental Validation of Axial Flow-Induced Vibrations on a Blunt-End Cantilever Rod for Nuclear Applications. *Arabian Journal for Science and Engineering* 50, 3435-3455 (**2025**). https://doi.org/10.1007/s13369-024-09505-5

[40] K. Zwijsen, S. Tajfirooz, F. Roelofs, A. Papukchiev, D. Vivaldi, H. Hadžić, S. Benhamadouche, W. Benguigui, T. Norddine, H. Iacovides, A. Cioncolini, M. R. A. Nabawy, K. Angele, E. Lillberg, B. Chazot, E. Iyamabo, Outcome of the VIKING project: status and perspectives of numerical modelling of flow-induced vibrations of nuclear power plant components. Nuclear Engineering and Design 440 (**2025**) 114131. https://doi.org/10.1016/j.nucengdes.**2025**.114131

[41] E. Bradley, H. Kantz, Nonlinear time-series analysis revisited, Chaos 25, 097610 (**2015**). https://doi.org/10.1063/1.4917289